Abstract

We propose to continue our study of $(e, e'p)$ reactions at high missing energies. A separation of the response functions $R_{\rm L}$ and $R_{\rm T}$ will be performed at $|\vec{q}| = 900$ MeV/c near $y = -200$ MeV/c (for ^{3,4}He) and at $|\vec{q}| = 685$ MeV/c, $y = +140$ MeV/c (for ^{4}He). The measurements will be made in parallel kinematics and will span the missing-energy range from the two-body breakup peak to about 100 MeV. When coupled with our previous data at $y = 0$ (on ^{3,4}He) and $+140$ MeV/c (^{3}He), these data will provide insights into the mechanisms responsible for the anomalously large strength seen in $(e, e'p)$ reactions at high missing energies. At $y \sim -200$ MeV/c we expect to be able to observe short-range correlations in the initial nuclear wavefunctions, without the complications due to isobar or meson-exchange currents.

1 Introduction

Studies of nuclei via the $(e,e'p)$ reaction have provided many insights into nuclear structure and dynamics in the past decade. While much is presently understood about this reaction, there are kinematical situations in which the currently-available data are not understandable in terms of any of the available models. Of particular interest to us are the reaction mechanisms and nuclear dynamics responsible for producing strength at large missing energies in $(e,e'p)$ reactions. We presented a review of the relevant literature in our original proposal [1]. Here we present a short summary of the relevant physics and the scientific motivation for the proposed experiment.

Many electron-induced proton knockout studies have been carried out at high missing energies and momenta, with the original goal of finding the single-particle strength which was "unexpectedly missing" [2] from the experimental phase space region $E_m < 20$ MeV and $|\vec{p}_m| < 250$ MeV/c. Short-range correlations (SRC) are generally thought to be at least partially responsible for this missing strength, since the "expected" strength being compared to is computed in the independent-particle shell model.

$(e,e'p)$ experiments on ^{4}He [3] and ^{12}C [4–7] have found unexpectedly large cross sections for knockout to high ($E_m > 50$ MeV) missing energies. A decomposition of the ^{12}C$(e,e'p)$ cross section into longitudinal and transverse responses $R_{\rm L}$ and $R_{\rm T}$ was performed at MIT/Bates [8] to investigate how this strength is generated. The longitudinal and transverse responses should be equal if the mechanism is initial-state correlations (SRC) or final-state interactions; for some other processes (e.g., meson-exchange currents) they would differ. $R_{\rm L}$ and $R_{\rm T}$ are indeed equal up to the two-nucleon emission threshold, above which the transverse response is enhanced. Similar results have been obtained for ^{6}Li [9], ^{10}B [10], and ^{12}C [11] at NIKHEF. In [8], for $E_m > 50$ MeV the strength is essentially completely transverse, and it persists out to the highest measured missing energies. These data all point to the existence of an unknown, primarily transverse, multi-body current.

Inclusive quasielastic (e,e') studies also have a bearing on this high-E_m puzzle. Extractions of $R_{\rm L}$ and $R_{\rm T}$ have been performed in order to investigate SRC effects via the Coulomb Sum Rule. This rule predicts a fairly model-independent relationship between the energy-integrated longitudinal response in (e,e') to the two-proton density (correlation) function [12]. Also, a y-scaling analysis of ^{3}He(e,e') cross sections has been shown [13] to be sensitive to two-nucleon correlation effects.

These various (e,e') experiments encountered anomalous results, which can be summarized as follows:

– although $R_{\rm L}$ and $R_{\rm T}$ scale separately in y, theoretical predictions of $R_{\rm T}$ consistently undershoot the data for all nuclei studied, with the exception of ^{3}He. The $R_{\rm L}$ predictions agree with the data, however.
– response in the "dip" region, between the peak due to quasielastic ep scattering and that due to excitation of the Δ resonance, is larger than theoretically predicted.

Many extensions have been made to the simple theory of electroproton knockout in an attempt to explain these phenomena. They usually fall under the broad categories of

– inclusion of meson exchange currents,
– inclusion of Δ and other isobar currents, and
– improvements in the final-state interaction between the proton and residual $A-1$ system.

Effective two-body currents due to meson exchange have been shown [14] to resolve the inclusive ^{3,4}He (e,e') L/T scaling puzzle, but they do not attempt to explain the unseparated $(e,e'p)$ results for ^{4}He or ^{12}C. Calculations for $(e,e'p)$ which include these MEC and isobar-current effects underpredict the data substantially, especially in parallel kinematics and at the highest missing energies [15–17]. There has been less progress in the improvement of final-state treatments, but exploratory work has exacerbated the situation. It has been shown that uncertainties due to final-state effects are the smallest in parallel kinematics [18], but this is precisely where the worst agreement is seen between theory and experiment for high E_m.

The lack of relevant, high-quality systematic studies, especially for simple and calculable systems such as ^{3,4}He, has been a hindrance to theoretical progress in elucidating the nature of the high-energy components in nuclei. Our group proposed in 1993 [1] to perform just such a systematic high-quality study. We proposed to study the reactions ^{3,4}He$(e,e'p)$ at high missing energies and momenta, and at energy transfers ω which cover the quasielastic peak as well as regions 100–150 MeV above and below the peak. The measurement plan includes a separation of the longitudinal and transverse responses $R_{\rm L}$ and $R_{\rm T}$. This plan addresses the following questions:

– **What mechanism is responsible for the high-E_m strength?** We measure the same region of $(|\vec{q}|, E_m, p_m)$ in both the longitudinal and transverse kinematics, and for three separate $(y, |\vec{q}|)$ settings. The various possible mechanisms for generating strength at high E_m differ both in their relative longitudinal and transverse contributions, and their dependence on y. We believe that exploitation of these experimental "handles" will enable us to discover the primary mechanism for producing the high-E_m yield.
– **What mechanism is responsible for the L/T discrepancy?** We will

study how the L/T separation for $(e, e'p)$ evolves with y, and E_m, and we will investigate both ^{3}He and ^{4}He since their inclusive responses $R_{\rm L}$ and $R_{\rm T}$ are so different in character.

- **Is there any sign of short-range correlations?** Using the systematics of our measurements, we hope to identify and control the "contaminant" processes (interesting in their own right) and to be able to make a clear statement about the presence or absence of SRC effects. In the context of the present measurements, it is more proper to speak of finding experimental signatures of the short-range nuclear force. By SRC one usually means that part of the nuclear wavefunction which is omitted due to the independent-particle assumption, but most modern calculations for $A = 3{,}4$ are fully many-body in nature.
- **Is the strength at high E_m consistent with our current theoretical understanding, or is new physics necessary?**

One final aside on kinematic conventions: we refer often to the scaling variable y in this proposal. It indicates the *minimum* struck-proton momentum that is probed in a given kinematical setup; $y = 0$ thus corresponds to probing the quasielastic peak in the (e, e') response. Negative y values correspond to $\omega < q^2/2m_N$. There are several definitions in the literature, some of which are incorrect.

We use the following definition [19]:

$$y(q, \omega) = \left[(M_A + \omega)\sqrt{\Lambda^2 - M_{A-1}^2 W^2} - q\Lambda\right] / W^2 \qquad (1)$$

where M_A is the target nucleus mass, M_{A-1} is the ground-state mass of the residual nucleus,

$$W = \sqrt{(M_A + \omega)^2 - q^2}$$

is the total center-of-mass energy, and

$$\Lambda = (M_{A-1}^2 - M_{\rm nucleon}^2 + W^2)/2$$

2 Experimental Technique

The measurements will be performed using the precision three-spectrometer system in the A1 Hall at MAMI. The general measurement program will follow what has been outlined in our original proposal [1] and elaborated upon in our addendum to the proposal [20] which detailed the control of systematic errors.

In general, a measurement of the longitudinal and transverse structure functions involves a Rosenbluth separation. The $(e,e'p)$ cross section in parallel kinematics is

$$\frac{d^6\sigma}{dE_{e'}d\Omega_{e'}dE_x d\Omega_x} = K\sigma_{\mathrm{Mott}} v_L \left[R_L + (v_T/v_L)R_T\right], \tag{2}$$

where e' and x refer to the emitted electron and proton [21]. The kinematic function

$$v_L = \frac{Q^4}{q^4} \tag{3}$$

remains fixed if q and Q remain fixed, but

$$v_T = \frac{Q^2}{2q^2} + \tan^2\frac{\theta}{2} \tag{4}$$

is dependent on the electron-scattering angle θ_e.

A Rosenbluth separation is performed by making measurements at several combinations of beam energy and electron scattering angle, such that q and ω (and thus also Q^2) are kept fixed. The individual measurements then have the same v_L but different v_T. R_L and R_T are extracted by fitting a line on a plot of σ vs. v_T. The slope and intercept are proportional to R_T and R_L.

Systematic errors must be kept well under control; for a small number of data points, the extraction is essentially a subtraction, so the relative errors on R_L and R_T are larger than those on the contributing cross sections. The most significant systematic uncertainties have to do with acceptances of the spectrometers and with absolute normalization of the data.

2.1 Spectrometers

Spectrometers A and B will be used to detect the scattered electrons and emitted protons. The spectrometer extended-target acceptances have been studied in a dedicated experiment. A natural carbon target was mounted on a movable table at the spectrometer pivot, and ^{12}C(e,e) elastic scattering was measured at 45^o. This measurement was repeated at several values of y_{target}, which is the distance along the beam direction between the spectrometer pivot point and the beam-target interaction point. In this way, we probed the spectrometer acceptance over the y_{target} range spanned by the target used in the real measurement.

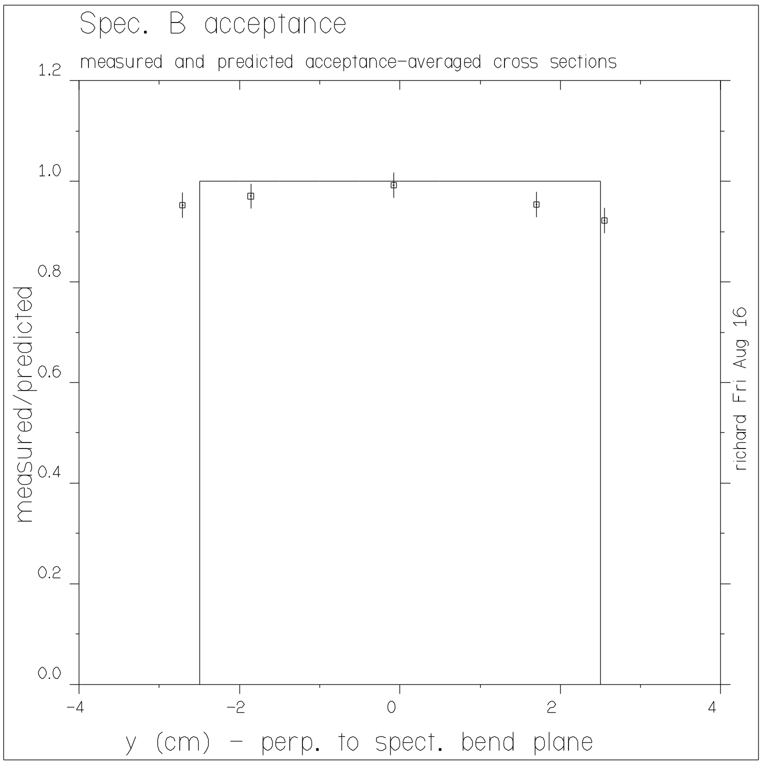

Fig. 1. Plot of the ratio of measured ^{12}C elastic cross sections to "theoretical" predictions, as a function of target position. A ratio of 1 means perfect agreement between the two. The box drawn between -2.5 and +2.5 cm depicts the design limits on the y_{target} region where 100% acceptance can be expected.

Fig. 1 shows the results of an *absolute* determination of the efficiency for spectrometer B, which tests our understanding of the spectrometer detectors, the beam charge integration, and the spectrometer's $y_{\text{target}} = 0$ acceptance. It also measures the extended-target acceptance. The efficiency is plotted as a function of y_{target}. The efficiency value of 1 at $y_{\text{target}} = 0$ implies perfect agreement between the radiatively-corrected experimental cross section and the value predicted from a calculations using a model-independent analysis of the ^{12}C charge density.

2.2 Absolute Normalization

The target for our experiment is a spherical cell containing cryogenic gaseous helium. The pressure and temperature of the gas is monitored continuously. However, the monitors are not (and cannot be) located in the beam path, and the heating in the target due to the enormous beam power of MAMI means that the thermodynamic state and properties of the target gas vary with the distance from the beam. Thus it is not possible to reliably compute the gas density from the pressure and temperature measurements. Therefore we take a different tack, and devote one detector (Spectrometer C) to continuous monitoring of the luminosity. Due to spatial constraints, Spectrometer C must be at a back-angle setting; the fields are set for detection of quasielastic electron scattering.

We measure the "conversion constant" of the spectrometer several times during the experiment. Elastic scattering data are taken (for kinematic regions where the cross section for elastic scattering is known to a couple of percent) and these can be used to determine the target density through the known cross sections and beam charge integration. The counting rate in Spectrometer C is in this way tied to the product of target density and beam current.

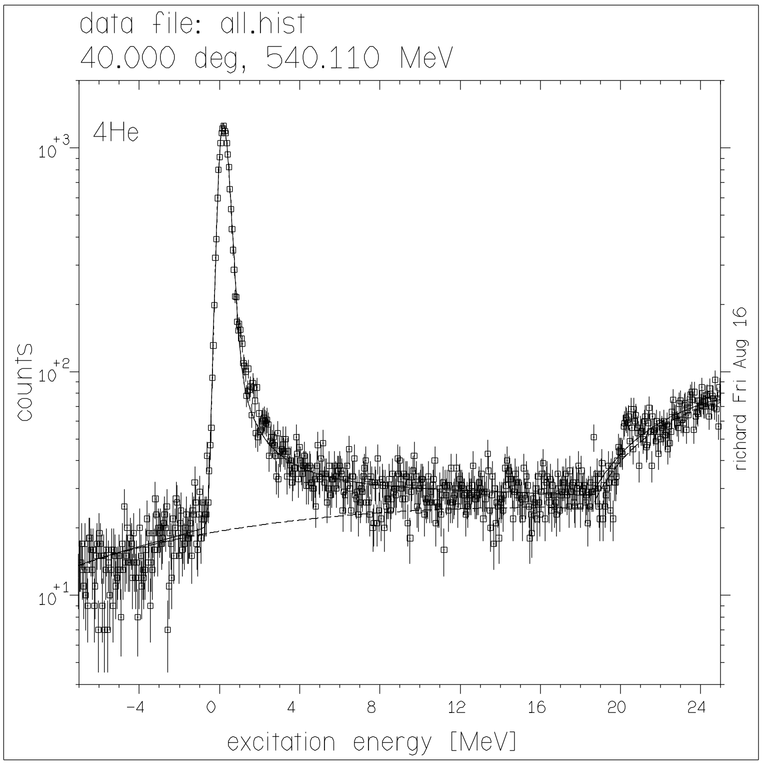

Fig. 2. Excitation-energy spectrum for scattering from ^{4}He by 540 MeV electrons. The ingredients in the calculation of the curve are discussed in the text.

Figure 2 shows the spectrum of electrons scattered from ^{4}He for one of these Spectrometer-C calibration runs. The x axis is the excitation energy of the recoiling $A = 4$ system. The large peak is due to elastic electron scattering from ^{4}He. The solid curve is a fit to the spectrum, which accounts for both the energy resolution of the spectrometer and radiative effects. Background contributions from quasielastic scattering from the iron walls of the target cell, and from the ^{4}He target, are included.

This spectrum fit is used to extract the elastic scattering rate from the ^{4}He gas, which in turn is combined with the known cross sections to determine the target density. The result is within 10–20% of the density predicted from the temperature and pressure measurements. Better agreement cannot be expected, since local effects of beam heating change the gas properties in the beam-interaction region, while the calculation can only determine the properties in the region away from the beam.

2.3 Preliminary Results

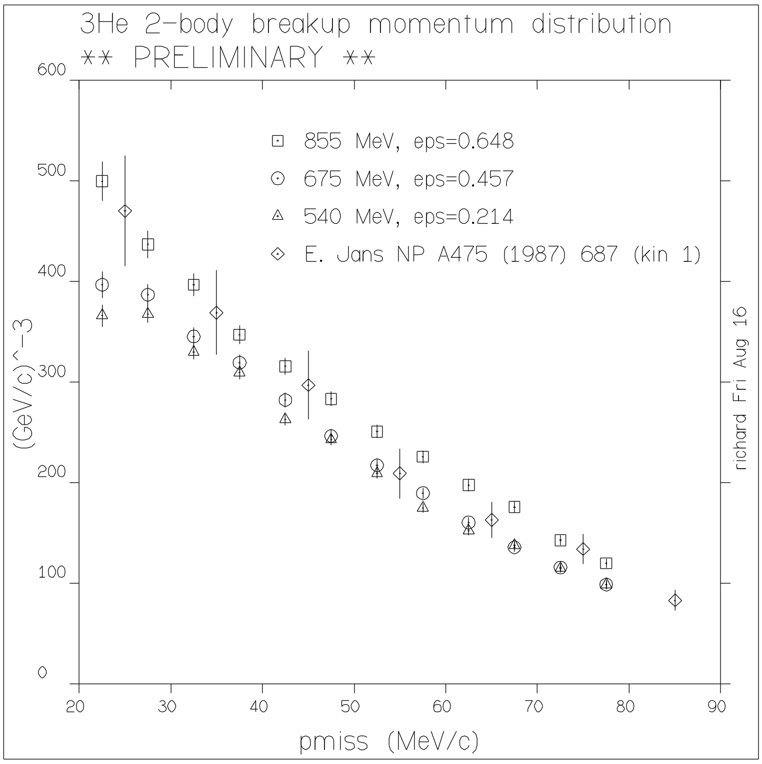

Fig. 3. Preliminary results for the distorted momentum distribution of protons in ^{3}He, measured at Mainz in 1995 via the reaction $^3\mathrm{He}(e,e'p)^2\mathrm{H}$. The three data sets correspond to measurements at electron beam energies of 540, 675, and 855 MeV, respectively. Results measured at NIKHEF [22] are also presented for comparison.

To illustrate the quality of the data being obtained, we show preliminary results for the distorted momentum distributions for the two-body breakup reaction $^3\mathrm{He}(e,e'p)^2\mathrm{H}$ in figure 3. Even at this early stage of the analysis, the internal consistency of the data and agreement with published results is impressive. We expect first results for the L/T separation of these data to be available before the end of 1996.

3 Current Status of the Program

In the past year, we have executed a substantial part of this measurement program. In summer 1995, we measured the $y = 0$ part (on the quasielastic peak) of the program. The L/T separation of the data for both ^{3}He and ^{4}He forms the PhD thesis work of MIT student R. Florizone. We also measured the $R_{\rm LT}$ response in ^{4}He$(e, e'p)^3$H over the missing-momentum range $150 \leq p_m \leq 300$ MeV/c. In the summer of 1996, we measured the longitudinal and transverse responses at positive y for ^{3}He, as well as the response function $R_{\rm LT}$ in ^{3}He$(e, e'p)^2$H. Table 1 summarizes the complete measurement program originally proposed, and shows the status of each part.

Nucleus	Data	Kinematics (MeV/c)	Status (Date)
^{3}He	$R_{\rm L}$, $R_{\rm T}$	$(y, q) = (0, 685)$	DONE (Jun 1995)
^{4}He	$R_{\rm L}$, $R_{\rm T}$	$(y, q) = (0, 685)$	DONE (Jul 1995)
^{4}He	$R_{\rm LT}$	$100 \leq p_m \leq 300$	DONE (Jul 1995)
^{3}He	$R_{\rm LT}$	$100 \leq p_m \leq 300$	DONE (Aug 1996)
^{3}He	$R_{\rm L}$, $R_{\rm T}$	$(y, q) = (+140, 685)$	DONE (Sep 1996)
^{4}He	$R_{\rm L}$, $R_{\rm T}$	$(y, q) = (+140, 685)$	TO DO
^{3}He	$R_{\rm L}$, $R_{\rm T}$	$(y, q) = (-200, 900)$	TO DO
^{4}He	$R_{\rm L}$, $R_{\rm T}$	$(y, q) = (-200, 900)$	TO DO

Table 1
Summary of the measurement program proposed in [1] and the status of each component as of September 1996.

3.1 L/T Separations at $y = 0$

Our first measurements were taken at the peak of the quasielastic response. To the extent that the $(e, e'p)$ reaction mechanism is not substantially modified from the PWIA, this kinematical situation emphasizes that portion of the nuclear response due to single-nucleon currents. Data were measured at $|\vec{q}| = 685$ MeV/c and $\omega = 228$ MeV for missing energies up to approximately 150 MeV. This measurement was performed in parallel kinematics at three beam energies (540, 675, and 855 MeV) which correspond to virtual photon polarizations ϵ of (0.21, 0.45, 0.64), or equivalently $v_T/v_L = (2.7, 1.25, 0.87)$. At each beam energy, both ^{3}He and ^{4}He data were taken. Table 2 shows a summary of the measurements performed at $y = 0$.

These data are currently being analyzed at MIT. Great progress has been

E_i (MeV)	E_f (MeV)	θ_e (deg)	v_T/v_L	θ_p (deg)
Data for ^{3}He				
540	311.6	103.85	2.63	26.21
675	446.6	72.05	1.23	38.33
855	626.6	52.36	0.868	46.41
Data for ^{4}He				
540	297.3	106.14	2.89	24.64
675	432.3	72.73	1.28	37.06
855	612.3	52.55	0.890	45.20

Table 2
Summary of $y = 0$ measurements made in 1995. Central kinematic values are listed. At each beam energy, four different settings of the proton momentum are used, each probing a different (E_m, p_m) region. The data cover a missing energy range $0 \leq E_m \leq 150$ MeV.

made in understanding the apparatus and controlling systematic errors. This is quite important for an L/T separation program, since small systematic relative errors between the individual measurements at each (v_T/v_L) are amplified when extracting $R_{\rm L}$ and $R_{\rm T}$.

Some preliminary results of this program are discussed in section 2.3, in the context of systematic error control.

3.2 L/T Separation at $y = +140$ MeV/c

We have measured the structure functions $R_{\rm L}$ and $R_{\rm T}$ for $^3{\rm He}(e, e'p)$ at $y = +140$ MeV/c in August of 1996. This value of y corresponds to a point halfway down the high-energy side of the quasielastic peak as measured by (e, e') [21]. Comparing to the $y = 0$ data, at $y = +140$ MeV/c we expect the responses (especially $R_{\rm T}$) to be more sensitive to details of multi-body effects such as virtual excitation of the Δ resonance (leading to two-body knockout) as well as meson-exchange currents. With the beam time available in summer 1996, we were able to carry out the separation for ^{3}He. The equivalent separation on ^{4}He comprises part of the measurement program proposed in this document.

Table 3 contains a summary of the kinematics for the ^{3}He separation at $y = +140$ MeV/c. It also includes a short exploratory measurement at $y = -190$ MeV/c. This measurement was done in order to test how accurately we can

E_i (MeV)	E_f (MeV)	θ_e (deg)	v_T/v_L	θ_p (deg)
$y = +140$ MeV/c Data				
570	248.1	107.03	3.65	20.26
675	353.1	76.54	1.67	30.08
855	533.1	53.21	1.05	38.55
$y = -190$ MeV/c Data (exploratory)				
855	603.2	73.9	1.21	40.10
675	423.0	107.9	2.77	26.53

Table 3
Summary of L/T separation measurements made in 1996. Only ^{3}He data were acquired. Central kinematic values are listed. For the $y = +140$ MeV/c data, two different settings of the proton momentum are used. The missing energy ranges spanned are $0 \leq E_m \leq 150$ MeV ("$+y$") and $0 \leq E_m \leq 80$ MeV ("$-y$").

estimate the count rates at negative y and will be reflected in our final run plan for the negative-y experiments.

3.3 Extraction of the $R_{\rm LT}$ Interference Structure Function

One addendum to our original proposal concerns the measurement of the structure function $R_{\rm LT}$ for ^{4}He$(e,e'p)^3$H. We made this measurement in 1995, and in 1996 made an $R_{\rm LT}$ extraction for ^{3}He$(e,e'p)^2$H as well. Our main interest in the extraction of $R_{\rm LT}$ is the observation [23–25] that it is very sensitive to two-body currents in the nucleus. Since multibody effects appear to play a central role in both the $(e,e'p)$ L/T discrepancy and the ^{3,4}He(e,e') L/T differences, we have measured $R_{\rm LT}$ for both nuclides.

Table 4 shows a summary of the measurements we've performed on $R_{\rm LT}$ for both ^{3}He and ^{4}He. Note that these measurements are performed in quasiperpendicular kinematics, since $R_{\rm LT}$ vanishes as one approaches parallel kinematics. Analysis of these data is in progress at California State University at Los Angeles.

p_m (MeV/c)	p_p (Mev/c)	$E_{\rm beam}$ (MeV)	θ_e (deg)	θ_q (deg)	θ_p (deg)
150	608.5	675	55	-43.2	-56.78
				-43.2	-29.65
200			50	-43.7	-62.26
				-43.7	-25.01
260			36	-42.7	-60.41
				-42.7	-25.01
300	550.0	855	47.7	-50.8	-76.70
				-50.8	-25.01

Table 4
Summary of $R_{\rm LT}$ measurements made in 1995 and 1996. Data at each kinematic point have been measured for both ^{3}He and ^{4}He.

4 Completion of the Program: Proposed Measurements

This proposal details our plans to complete the measurements identified as "to do" in table 1. It includes the ^{4}He dataset at $y = +140$ MeV/c, and the full L/T separation program for both helium nuclides at $y = -200$ MeV/c.

Our interest in the physics of these two data sets was outlined in the introduction. The data at $y = -190$ MeV/c warrants a bit more discussion, as we have chosen a different three-momentum transfer, $q = 900$ MeV/c, for this part of the program than for the other two parts. This choice is driven by our interest in obtaining the best possible information on *initial-state* two-body correlations in the nucleus. The inclusive y-scaling analysis of Sick *et al.* [13] claimed that the effect of two-body correlations could be observed if $q \geq 900$ MeV/c and $y \leq -190$ MeV/c. This claim motivates our choice to raise the momentum transfer for this part of the program, and to use a "$-y$" value with a different absolute value than "$+y$".

The negative-y program also encounters the lowest cross sections of the entire program. We have adjusted this part of the measurement to reduce the amount of time necessary by covering a smaller range in (E_m, p_m). We defer a decision whether to pursue the higher (E_m, p_m) data until the current measurement is completed and we can evaluate whether the predicted rates are realistic. We urge the PAC to approve the full request of this program in spite of the large amount of time requested, as the physics payoff is expected to be large.

4.1 Kinematical Settings

Table 5 lists the proposed kinematical settings for the $y = +140$ MeV/c measurement (referred to hereafter as "$+y$".) They have been chosen so that the central y value is the same, and the virtual photon momentum (q, ω), missing-energy and -momentum ranges are as close as possible, to those of the August/September 1996 measurements on ^{3}He. Note that for all the proposed measurements, we will use spectrometer A for detection of electrons, and spectrometer B for proton detection.

Electron Arm				Proton Arm	
E_{inci} (MeV)	θ_e (deg)	p_e (MeV/c)	v_T/v_L	θ_p (deg)	p_p (MeV/c)
570	109.22	236.09	3.6	18.99	790
					700
					610
675	77.11	341.09	1.7	29.04	790
					700
					610
855	53.23	521.09	1.05	37.55	790
					700
					610

Table 5
Summary of the kinematical settings for the proposed L/T separation on ^{4}He at $y = +140$ MeV/c. Central kinematic values are listed. The values of the L/T separation parameter v_T/v_L and the E_m coverage are essentially identical to those of table 3.

The kinematical settings for the proposed measurements at $y \sim -200$ MeV/c (hereafter referred to as "$-y$") are listed in table 6. Here we have chosen not to keep y the same between the ^{3}He and ^{4}He data sets, but rather to use the maximum possible electron-scattering angle for each data set in order to optimize the L/T separation lever arm. This results in (q, ω) being identical between the two, but y values of -193 MeV/c for ^{3}He and -214 MeV/c for ^{4}He. This optimization is important due to the expected low counting rates at $-y$. The kinematic coverage in (E_m, p_m) of the $-y$ program is shown graphically in figure 4.

Electron Arm				Proton Arm	
E_{inci} (MeV)	θ_e (deg)	p_e (MeV/c)	v_T/v_L	θ_p (deg)	p_p (MeV/c)
600	142	348	10.47	-13.8	650 (555)
705	100	454	2.20	-29.8	650 (555)
855	74	603	1.21	-40.1	650 (555)

Table 6
Summary of the central kinematic settings for the proposed "$-y$" measurements for ^{3,4}He. These kinematics yield $y = -193$ MeV/c for ^{3}He and $y = -214$ MeV/c for ^{4}He. The settings in parentheses are for a possible "bite" at higher (E_m, p_m), but are not part of the current proposal.

4.2 Count Rate Estimates

All the required-time and count-rate estimates presented here assume the "standard" running conditions for our setup in A1: a beam current of 30 μA and a helium cryotarget pressure of 14 atmospheres. This yields a luminosity factor of approximately 2.6×10^{36} s^{-1}cm^{-2} (average of ^{3,4}He.)

Rate estimates for the $y = +140$ MeV/c measurement on ^{4}He can be gained directly from the August/September 1996 measurements on ^{3}He. The data from the 1995 experiment at y=0 showed that the counting rates from the two-body breakup channels of ^{3}He and ^{4}He are comparable. Lacking a detailed spectral function for ^{4}He, we estimate that time required for the ^{4}He measurement at $+y$ to be the same as that for the comparable ^{3}He data. These estimates are summarized in Table 7. We expect the time requested to be sufficient to obtain a statistical precision, for each 10 MeV bin in the E_m range $0 \leq E_m \leq 100$ MeV, of better than 2%. This precision was obtained for the ^{3}He $+y$ experiment.

The rate estimates for the $y = -193$ MeV/c program on ^{3}He were calculated using the same procedure described in our last PAC submission [20]. The ^{3}He spectral function used is due to I. Sick [26]. The Monte-Carlo program MCEEP [27] did the necessary kinematic and detection-volume calculations, along with generating the $(e, e'p)$ cross sections from the spectral function. The rates are displayed in table 8 for the forwardmost (at $E_{\text{inci}} = 855$ MeV) and most backward (at $E_{\text{inci}} = 600$ MeV) electron angles.

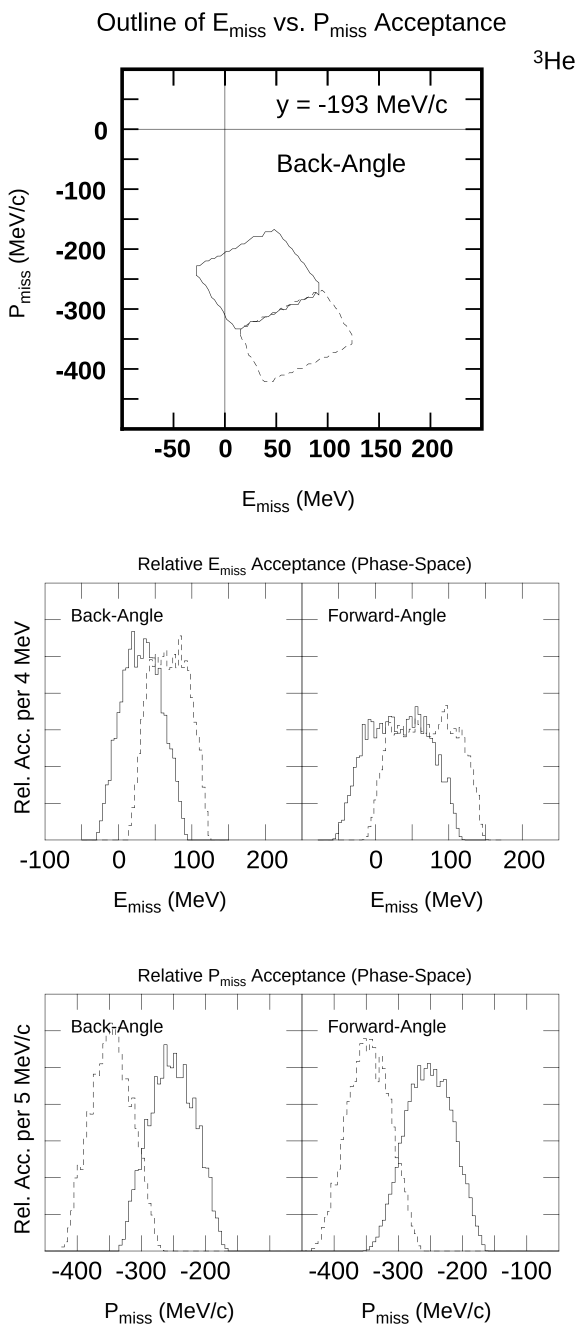

Fig. 4. Phase-space acceptance of the proposed coincidence measurement for ^3He at the $y = -193$ MeV/c kinematics. The "back angle" plots are the acceptances obtained for the $E_{\text{inci}} = 600$ MeV kinematics, and the "forward angle" are for $E_{\text{inci}} = 855$ MeV. The solid lines show the acceptance for the $P_p = 650$ MeV/c setting, and the dashed for a possible future high-E_m extension at $P_p = 555$ MeV/c.

A preliminary analysis of the exploratory $-y$ measurement at $E_{\text{inci}} = 675$ MeV yielded a counting rate of 35 hr^{-1} in the missing energy bin $40 \leq E_M < 80$

Kinematical Setting		Time
E_{inci} (MeV)	p_{proton} (MeV/c)	Required (hours)
570	790	9
	700	20
	610	6
675	790	7
	700	15
	610	4
855	790	6
	700	11
	610	2

Table 7
Time Estimates for ^{4}He y=+140 MeV/c (based on previous ^{3}He data). Assumes same running conditions as our 1996 run (see text).

MeV. The predicted rate for the same E_m region at E_{inci} = 600 MeV is 24 hr^{-1}. Since the kinematic variables y, q, Q^2, and p_p are the same for both the exploratory measurement and the E_{inci} = 600 MeV kinematical setting, R_{L} and R_{T} are expected to be constant and the expected change in cross section can be simply computed from eqn. 2. For purely-longitudinal and purely-transverse processes, we find $\sigma_{675}/\sigma_{600}$ to be 3.6 and 1.0 respectively. The ratio $\sigma_{675}^{\text{measured}}/\sigma_{600}^{\text{predicted}}$ is 1.5. This analysis suggests that our predicted rates are within a factor of two of those we will encounter. The implication is that our beam-time request is reasonably realistic.

The second proton-momentum bite, which would have covered a phase space region of higher E_m and p_m, is predicted to take a prohibitively large amount of beam time. We do not request time for this measurement in the current proposal. If the $-y$ measurements proposed here indicate that the true rates are much larger than the predictions, we will submit an addendum concerning these data. We do not discuss it further in this proposal.

These considerations lead to the beam-time request for the $-y$ program on ^{3}He shown in table 9. For the first proton-momentum setting (corresponding to $0 \leq E_m \leq 80$ MeV), we require a statistical uncertainty of 2% or better per 10 MeV bin for all $E_m \leq 50$ MeV. At the second momentum setting ($50 \leq E_m \leq 130$ MeV), we double the bin size, *i.e.,* a 2% statistical uncertainty per 20 MeV bin. These criteria are roughly the same as were discussed in [20].

	$p_{\mathrm{proton}} = 650$ MeV/c		$p_{\mathrm{proton}} = 555$ MeV/c	
$\mathrm{E_{inci}} \rightarrow$	855 MeV	600 MeV	855 MeV	600 MeV
E_m (MeV)	Coincidence Rate (hr^{-1})			
20–30	111.900	30.825	0.525	1.050
30–40	57.675	19.050	1.950	2.100
40–50	36.225	12.900	2.250	2.175
50–60	25.800	6.750	1.800	1.650
60–70	17.175	3.000	1.125	1.275
70–80	9.525	1.125	0.750	0.900
80–90	3.975	0.300	0.525	0.600
90–100	1.650	0.007	0.300	0.450
100–110	0	0	0.150	0.225
110–120	0	0	0.075	0.075

Table 8
A summary of the predicted coincidence rates for ^{3}He at $y = -193$ MeV/c kinematics for the most forward and most backward electron angles. Note that the forward-angle rates have accounted for matching the detection volume in q and ω with that of the backward-angle data. The same luminosity is assumed as for table 7.

Kinematical Setting		Time
E_{inci} (MeV)	p_{proton} (MeV/c)	Required (hours)
600	650	190
	555	(860)
705	650	130
	555	(860)
855	650	70
	555	(860)

Table 9
Time Estimates for ^{3}He at $y \sim -200$ MeV/c The estimates assume that the luminosity is the same as for the 1996 run (see text). The beam time at $E_{\mathrm{inci}} = 705$ MeV has been chosen as the average of that of the other two energies. The times in parentheses show the estimated time for a second proton-momentum bite, but time for this bite is not part of the current proposal.

Kinematics		Singles				Accidentals
E_{inci} MeV	$\mathrm{P}_{\mathrm{proton}}$ (MeV/c)	(e,e') (kHz)	(e,π^-) (kHz)	(e,p) (kHz)	(e,π^+) (kHz)	(e,e'p) (hr^{-1})
^{3}He: y = -193 MeV/c						
600	650	0.021	0.000	1.042	0.000	0.16
	555	0.021	0.000	1.233	0.262	0.19
855	650	0.087	0.000	1.051	0.131	0.66
	555	0.087	0.000	1.430	0.677	0.90
^{4}He: y = -214 MeV/c						
600	650	0.015	0.000	1.371	0.000	0.15
	555	0.015	0.000	1.535	0.197	0.17
855	650	0.064	0.000	1.448	0.099	0.67
	555	0.064	0.000	1.914	0.526	0.88

Table 10
Estimated singles and accidental-coincidence rates for the "$-y$" kinematical settings. The luminosity assumed is the same as for table 7, and a coincidence resolving time of 2 ns was applied. Note that no E_{miss} cut has been applied to the accidental coincidence rate.

Using the arguments put forward on page 15 (for the "$+y$" program), we request the same amount of time for both the ^{3}He and ^{4}He measurements.

5 Singles Counting Rates and Accidental Coincidences

The singles counting rates observed in Spectrometer A originating from (e,e') and (e,π^-) reactions, those in Spectrometer B originating from (e,p) and (e,π^+) reactions, have been estimated with the help of the codes QFS and EPC of Lightbody and O'Connell [28]. The estimated rates correspond to the computed reaction cross sections which span the full acceptance of each spectrometer. The singles-rate results for the $-y$ kinematical settings are shown in table 10.

The level of accuracy of these estimates is uncertain. The same estimation procedure was quite successful for the $y = 0$ measurement — the measured rates were within 30% of the predictions. However, the singles rates during the the $y = +140$ MeV/c runs were typically 5–7 times larger than predicted. More reliable singles rates will be extracted from the recently-acquired exploratory data in the $-y$ kinematical setting.

6 Additional Measurements and Overhead

The beam times listed above only concern the production-data measurement. There are several classes of additional measurements which are necessary in order to have a complete data set. We outline them briefly in this section.

6.1 Elastic-Scattering Data

As discussed in section 2.2, measurements of elastic scattering on helium are needed in order to normalize the production data. Our experience over the last two years has shown that the following program is sufficient to understand the data normalization:

- three elastic scattering runs, each at a different beam current but fixed scattering angle (investigate heating effect on density);
- one empty-target measurement in the elastic-scattering setup (measure cell-wall contribution);
- one elastic scattering run at a second scattering angle (systematic error check).

The total time needed for this program is 2.5 hours at each beam energy.

6.2 Empty-Target Measurements

We measure a sample of $(e, e'p)$ coincidences from an empty target in order to ascertain the cell-wall contributions to our He$(e, e'p)$ data. Most of the cell-wall contribution can be excluded by making cuts on the target reaction vertex as seen by the spectrometers, but there are tails from the cell walls which contaminate the "good" region of the target vertex. We make the empty measurement at low E_m to determine the ratio of counts inside the "good" region to the counts in the peaks which are seen due to the walls. We assume that this ratio is constant for a constant detection geometry, and then can use the measured number of counts in the cell-wall peaks for each helium run to predict the number of background counts in the helium data. Three hours at each beam energy and y setting is sufficient.

6.3 Assorted Calibration Measurements

Each year, we have found it necessary to make various "unexpected" calibration measurements. These usually fall into one of three classes:

– measurements to answer a question raised in the analysis of data from the previous year;
– measurements to fix the calibration of a spectrometer or detector in a previously-unused region of operation, or
– measurements to verify the calibration of a detector which has recently been repaired or replaced.

It is not possible to precisely specify the time which will be needed, but we have generally not needed more that twelve hours for this sort of work, which is what we request in this proposal.

6.4 Overhead for Energy/Angle Changes

For each beam energy change, we request a total of six hours. This time will be spent both in changing the beam energy of MAMI, as well as making a "big loop" in the electron-spectrometer fields and in changing the angles of both spectrometers.

7 Beam Time Request

Table 11 shows the total beam time requested to bring our program proposed in [1] to completion. The time listed for each component of the request includes the following items:

(i) the sum of the production-data time estimates listed in the tables above;
(ii) twelve hours for miscellaneous calibration measurements
(iii) twelve hours for two beam-energy changes and associated spectrometer-angle changes
(iv) seventeen hours total for elastic-scattering and empty-target measurements at each of the three beam energies used per component.

Experience dictates that one should expect that about thirty percent of the *real* time allocated will be lost to various equipment failures or problems. The numbers in the table above *do not* account for this factor. The numbers of hours above should be divided by 0.7 to compute how much real time should be allocated to the experiment.

Nuclide	Kinematics	Request (hr)
^{4}He	$+y$	120
^{3}He	$-y$	430
^{4}He	$-y$	430
Total		980

Table 11
Total beam time requested for this proposal. The computation is detailed in the text. The numbers do not include any contingency factor, which is estimated from past experience at 30%.

References

[1] Studies of the $(e, e'p)$ reaction at high missing energy, MAMI Proposal A1/1-93, 1993.

[2] L. Lapikás, Nucl. Phys. **A553**, 297c (1993).

[3] J. J. van Leeuwe et al., High missing-momentum components in ^{4}He studied with the $(e, e'p)$ reaction, in *Proceedings of the 15*$^{\mathrm{th}}$ *European Conf. on Few-Body Problems in Physics*, Peniscola, 1995.

[4] R. W. Lourie et al., Phys. Rev. Lett. **56**, 2364 (1986).

[5] L. B. Weinstein et al., Phys. Rev. Lett. **64**, 1646 (1990).

[6] L. J. H. M. Kester et al., Phys. Lett. **B366**, 44 (1996).

[7] J. Morrison et al., submitted to Phys. Rev. **C**.

[8] P. E. Ulmer et al., Phys. Rev. Lett. **59**, 2259 (1987).

[9] J. B. J. M. Lanen et al., Phys. Rev. Lett. **64**, 2250 (1990).

[10] L. J. de Bever, *A comparison of real and virtual photon reactions on* ^{10}B, PhD thesis, Rijksuniversiteit Utrecht, 1993.

[11] G. van der Steenhoven et al., Nucl. Phys. **A484**, 445 (1988).

[12] T. de Forest, Nucl. Phys. **A414**, 347 (1983).

[13] I. Sick, D. Day, and J. S. McCarthy, Phys. Rev. Lett. **45**, 871 (1980).

[14] J. Carlson and R. Schiavilla, Phys. Rev. **C49**, R2880 (1994).

[15] R. de Vries, *Investigation of nucleon-nucleon correlations in* ^{4}*He with the reactions* $(e, e'p)$ *and* $(e, e'pp)$, PhD thesis, Universiteit Utrecht, 1995.

[16] J. Ryckebusch, Invited Talk at Workshop on Short-Range Structure in Nuclei, CEBAF, 1996.

[17] J. J. van Leeuwe, *Investigation of Nucleon-Nucleon Correlations in ^4He*, PhD thesis, Universiteit Utrecht, 1996.

[18] A. Bianconi and M. Radici, Phys. Lett. B **363**, 24 (1995).

[19] D. Day, J. S. McCarthy, T. W. Donnelly, and I. Sick, Ann. Rev. Nucl. Part. Sci. **40**, 357 (1990).

[20] Addendum to Proposal A1/1-93, Submitted to the MAMI PAC, 1994.

[21] J. J. Kelly, Nucleon knockout by intermediate energy electrons, in *Advances in Nuclear Physics*, edited by J. W. Negele and E. Vogt, volume 23, page 75, Plenum Press, 1996.

[22] E. Jans et al., Nucl. Phys. **A475**, 687 (1987).

[23] M. Epstein et al., Phys. Rev. Lett. **70**, 2868 (1993).

[24] R. Schiavilla, Phys. Rev. Lett. **65**, 835 (1990).

[25] V. van der Sluys, J. Ryckebusch, and M. Waroquier, Phys. Rev. **C49**, 2695 (1994).

[26] I. Sick, private communication.

[27] P. E. Ulmer, computer program MCEEP, CEBAF Tech. Note 91-101, 1991.

[28] J. Lightbody and J. S. O'Connell, Computers in Physics **2**, 57 (1988).